

Computer simulation of a stable crack growth of a partly circumferential through crack in a pipe loaded by pure bending

C. Mattheck

*Kernforschungszentrum Karlsruhe, Institut für Festkörper- und Materialforschung IV,
FR Germany*

H. Moldenhauer

Ingenieurbüro, Rödermark, FR Germany

ABSTRACT

On the basis of a measured pipe end rotation - crack length relationship stable crack growth of a through the wall-crack is studied numerically. The J-integral is calculated using the line integral definition. It is shown that during the crack growth process a simple defined crack opening parameter is nearly constant with an error of about 5%. The crack growth is modeled by a simple numerical method which is not known from the literature after the authors knowledge.

1. INTRODUCTION

Whilst at load controlled conditions no or only small stable crack growth may happen in the case of displacement controlled conditions - for example under thermal loads - stable crack growth may increase the crack length by large amounts. The question is now which fracture mechanical parameter may be used to describe this phenomenon. In /1/ the problem of an edge cracked plate under axial tension is studied and an expression for the J-integral has been derived there. Further assumptions which include among others the assumption of a localized yielding region (hinge-like behaviour) allowed to apply this theory to circumferentially through cracked pipes under four point bending conditions /2/. The theory developed in /1/ has been applied in /3/ to experiments also with pipes under four point bending loads similar to that from /2,4/.

The method presented here does not use the analytical simplifications used in /1, 2/, only the line integral in its original definition is used.

2. DESCRIPTION OF THE MODEL

2.1 Idealisation of the geometry

The geometry of the cracked pipe studied experimentally in /3/ is given by:

Average pipe radius: $R = 28.85 \text{ mm}$

Wall thickness : $t = 2.6 \text{ mm}$

Length of the pipe : $l = 300 \text{ mm}$ (between rigid cylinders welded to both pipe ends during the four point bending experiments)

Initial crack limiting angle:

$$\varphi_0 = 69^\circ \text{ (with respect to } 360^\circ \text{ of full circumference)}$$

Fig. 1 shows the geometry idealized with 4-node shell elements as shown in Fig. 2. The zone of crack growth $69^\circ < \varphi < 229^\circ$ is idealized with 10 elements. That means the calculation is divided into ten steps. After every step the boundary conditions are redefined in the plane of symmetry $z = 0$ in order to simulate the crack growth. The free end of the pipe has been assumed to be rigid. The global moment as well as the rotation at the free pipe end can be obtained directly if any point of the pipe end is connected rigidly with the axis of the pipe which may be realized in the FE-program ABAQUS by use of so-called 'multi-point-constraints'.

The FE-grid in Fig. 2 contains a number of elements with a large aspect ratio (slender elements) which are nevertheless used here because their longer side is directed axially. This is also the direction of force flow under bending conditions. Therefore no steep gradients have to be expected there. At the pipe end with its long elements the stress gradient in axial direction is nearly zero. The maximum axial stress gradients near the crack have been considered by a much more refined grid in this region. Degenerated four-point elements or 'multi-point-constraints' which realize the connection of two elements to one element give results with reduced accuracy using ABAQUS /7/.

No doubt the idealization in Fig. 2 has too many degrees of freedom at the pipe end in circumferential direction. On the other hand the "super convergency" in shell elements with "reduced integration techniques", which has been used here can only be shown in a rectangular grid /7/.

2.2 MATERIAL PROPERTIES

The material studied was steel of the German designation 1.4541:

Young's modulus: $E = 2 \cdot 10^5 \text{ MPa}$

Poisson's ratio: $\nu = 0.3$

Hardening : see appendix describing the measured curves

The hardening as shown in the appendix is based on true stresses and technical strains ϵ_T . But ABAQUS requires the logarithmic strain ϵ_L , which is related to ϵ_T by

$$\epsilon_L = \ln (1 + \epsilon_T) \quad (1)$$

The computation carried out with ABAQUS has been nonlinear allowing unlimited large deflections and rotations, but some restrictions exist. The stress-strain-curve (Appendix) has been multilinearized using 25 linear subdivisions.

The strain in the present shell element is limited up to 5 %. Further straining initiates in the real shell a change of thickness which cannot be described by this type of shell element. This is one of the lacks of the present method but it is plausible that in the first stage of crack growth this restriction will not become dominant.

2.3 Loading

α is the rotation of pipe limbs with respect to the horizontal line.

α is prescribed at the free rigid end of the structure (Fig. 1). The moment-rotation-behaviour $M(\alpha)$ has been taken from the experiments in /3/. The moment-crack angle relation $M(\varphi)$ is also known from experiments. Combining this a measured $\alpha(\varphi)$ relation is known. This $\alpha(\varphi)$ -relation defines at which external rotation the boundary conditions in the plane of symmetry $z = 0$ (i.e. in the ligament of the crack) have to be modified in order to simulate the crack opening. For a given rotation ABAQUS calculates the related bending moment M_x (Fig. 1) from the stress distribution in the shell where the state of static equilibrium is realized. This calculated $M(\alpha)$ -curve will be compared with the measured curve from /3/ to check the quality of the simulation of the crack opening.

2.4 Boundary Conditions

The simulation of crack growth will be described now looking at the first step as an example. In the experiment /3/ the crack starts growing if the rotation has reached the value $\alpha = 2.52^\circ$. The first step of the calculation stops at this angle and yields the reaction forces at the crack tip, because they are situated in the plane of symmetry. Reaction forces mean here: a) One reaction force in z-direction. b) Two reaction moments with respect to the x- and y-axis. Before the next step with increasing externally prescribed rotation will be started the following intermediate step has to be inserted:

1. Redefinition of the boundary conditions at the crack tip. That means that the suppression of displacements in z-direction is released and the suppressed rotations about the x-axis and y-axis are released as well. All other boundary conditions in the ligament are not changed.

2. The reaction forces and moments calculated in the first step will be applied at the same node as an external loading.

3. The prescribed rotation is kept constant at 2.52° , that means in this intermediate step only a change from kinematic to static boundary conditions has happened.

4. Of course, the calculation with changed boundary conditions converges immediately because no real change in the loading has happened.

The second step defines now the rotations of the pipe end with respect to the $\alpha - \varphi$ -curve for $\varphi = 69^\circ + 16^\circ$. By the new definition of the crack tip in the intermediate step the tip has been shifted by an angle of 8° with respect to the half circumference. A discontinuity in the $M - \alpha$ -curve is avoided now by a linear decrease of the reaction force and moments down to zero whilst at the same time the externally prescribed rotation increment $\Delta\alpha$ is applied. This procedure is repeated for all crack tip shiftings during the whole simulation of the crack growth. The other symmetry conditions in the plane $x = 0$ and $z = 0$ suppress all degrees of freedom vertically directed to these planes. By this way also all rigid body movements are suppressed except the y-direction. Therefore the point ($x = 0, y = -R, z = 0$) is fixed which defines a reference point for the deflections. The reaction force in y-direction at this point vanishes during all steps because pure bending has been simulated.

3. CALCULATION OF THE J-INTEGRAL

For the case of plane stress conditions the J-integral /6/ is well known.

Not all requirements with respect to the applicability of the J-integral are satisfied in the case studied here. That means especially:

- The J-integral is only valid for membrane stresses.
- The J-integral is allowed to be used only in the situations before the start of stable crack growth.

Furthermore the large deformations are also a problem when evaluating it. However, there are some suggestions in /6/:

1. The stresses in the J-Integral are to be replaced by the nominal stresses (1st Piola-Kirchhoff-Stresses). The stresses in the output of ABAQUS are local stresses, i.e. the components of the stress tensor are rotating as required by the large displacements.

2. τ , μ , \bar{x} and \bar{y} are referred to the undeformed geometry.

3. The stress working is related to the initial volume.

An especially appropriate path of integration exists, which allows to compute the J-integral with less effort:

It is situated at the three borders of the FE-structure which are surrounding the crack tip (Fig. 3).

It should be mentioned critically that the present high strains are larger than the limit of 5 % valid for the shell elements. Also the large superimposed bending effects due to pipe bulging are subject of criticism with respect to the use of shell elements and the use of the J-integral itself. On the other hand, the use of three-dimensional elements which allow bending effects as well as higher strain would require unproportionally more computer time, striking modification of crack growth simulation without avoiding the 'misuse' of the J-integral. The bending stresses acting versus the wall thickness have to be eliminated in the stress tensor because in the J-integral only membrane stresses occur. Therefore a pipe surface inside the wall has been considered. It will be called here "membrane surface". This surface is not necessarily identical with the middle surface of the pipe wall, because the stress distribution versus the pipe wall may be nonlinear. None the less this membrane surface has been assumed to be the middle surface of the shell. This assumption is also in consistence with the use of the J-integral in this approximative manner. The membrane surface of the strain tensor is identical with the middle of the shell surface because of the linear strain assumption across the pipe thickness.

4. RESULTS

Fig. 4 shows the moment versus the bending angle. The agreement with the experiments from /3/ is very good. That means the crack opening simulation explained before is able to reproduce the measured $M(\alpha)$ curve by integrating the internal moment caused by the stresses in the pipe with satisfying agreement.

In Fig. 5 and Fig. 6 the J-integral is plotted in comparison with the results from /3/. Using the method described in section 3 the agreement is not satisfying.

One difference between the present theory and the results in /3/ is that in the present method no maximum in the J-curve occurs. This lack in agreement only at large crack growth length may be caused in the present theory by the limited accuracy of the shell elements at strains larger 5 %. On the other hand in /3/ a hingelike behaviour of the pipe is assumed.

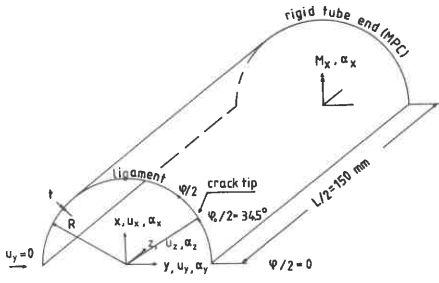
This assumption, that the plasticity will be limited locally on the ligament region is obviously not valid furthermore.

In addition the validity of the J-integral itself is limited basically to geometrical linear problems. It can be seen from Fig. 7 that all these assumptions are not valid when the crack has grown by large amounts. It cannot be judged from the present consideration whether the theory in /3/ or the present one becomes more wrong in this case.

Although the crack tip has been modeled neither with collapsed elements nor with a super-refined grid it can be seen from Fig. 8 that the crack opening at the first released node near the crack tip remains nearly constant. It is a question of opinion only to call this effect constant COD or constant COA (crack opening angle), but it seems that these generally spoken "crack opening parameters" are much less sensible also in the region of large crack increases. Further work should treat this good looking effect with elements allowing higher strains and a more refined crack tip which seem to be the only weak points of the COD-calculation presented here.

REFERENCES

- /1/ Ernst, H., Paris, P. & Landes, J. Estimation of the J-integral and tearing modulus T from a single specimen test record. Fracture Mechanics, 13. Conference, ASTM STP 743 (1981) 476-502.
- /2/ Zahoor, A. & Kanninen, M. Plastic fracture mechanics prediction of fracture instability in a circumferentially cracked pipe in bending. J. Press. Vess. Tech. 103, (1981) 352-358.
- /3/ Grunmach, R. Ausbreitung von Umfangsrissen in Rohren unter Biegebelastung. Doktorarbeit am Institut für Zuverlässigkeit und Schadenskunde der Universität Karlsruhe 1986.
- /4/ Brückner, A., Grunmach, R., Kneifel, B., Munz, D. & Thun, G. Fracture of pipes with circumferential cracks in four-point-bending. in: Wilkowski, G.M. Circumferential cracks in pressure vessels and piping, Vol. II, PVP-Vol. 95.
- /5/ Zahoor, A. Closed form expressions for fracture mechanics analysis of cracked pipes. J. Press. Vess. Tech. 107 (1985) 203-205.
- /6/ Rice, J., McMeeking, R., Parks, D. & Sorensen, E. Recent finite element studies in plasticity and fracture mechanics. Computer methods in applied mechanics and engineering 17/18 (1979) 411-442.
- /7/ Hibbitt, Karlsson & Sorensen. ABAQUS Example Problems Manual. Hibbitt, Karlsson & Sorensen. ABAQUS Theory Manual.



Symmetry conditions $z=0$ (ligament)
 $u_z = \alpha_x = \alpha_y = 0$
 Symmetry conditions $x=0$
 $u_x = \alpha_y = \alpha_z = 0$
 Rigid body movement $u_y(0, -R, 0) = 0$

Fig.1: Geometry and boundary conditions

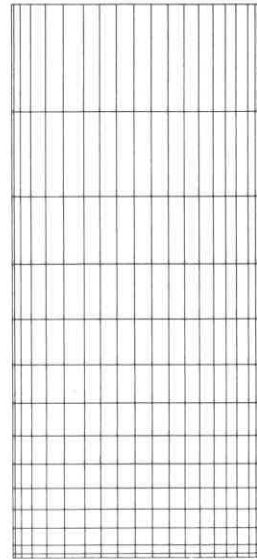
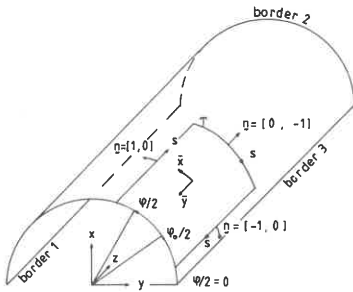


Fig.2: FEM-idealization used finally



$$J = 2 \int_{\Gamma} \left[\underbrace{W(\underline{\underline{\epsilon}})}_{\text{term 1}} \cdot \underline{n}_{\bar{x}} - \underbrace{\underline{n} \cdot \underline{g}}_{\text{term 2}} \cdot \partial \underline{u} / \partial \bar{x} \right] ds$$

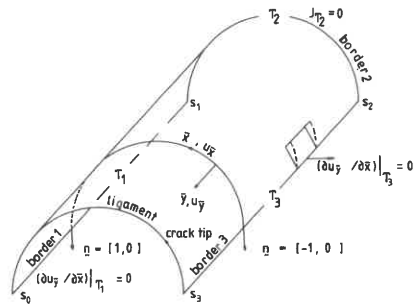
$$W = \int_0^{\underline{\underline{\epsilon}}} \underline{\underline{\sigma}} d\underline{\underline{\epsilon}}$$

$$\underline{n} = [n_{\bar{x}}, n_{\bar{y}}] \quad \underline{u} = \begin{bmatrix} u_{\bar{x}} \\ u_{\bar{y}} \end{bmatrix}$$

$$\underline{\underline{\sigma}} = \begin{bmatrix} \sigma_{\bar{x}\bar{x}} & \sigma_{\bar{x}\bar{y}} \\ \sigma_{\bar{y}\bar{x}} & \sigma_{\bar{y}\bar{y}} \end{bmatrix} \quad \underline{\underline{\epsilon}} = \begin{bmatrix} \epsilon_{\bar{x}\bar{x}} & \epsilon_{\bar{x}\bar{y}} \\ \epsilon_{\bar{y}\bar{x}} & \epsilon_{\bar{y}\bar{y}} \end{bmatrix}$$

\bar{x}, \bar{y} : local system in the middle plane of the shell

Fig.3a: Definition used for the calculation of the J-integral



$$J_{T_1} = \int_{s_0}^{s_1} (W - \sigma_{\bar{x}\bar{x}} \cdot \partial u_{\bar{x}} / \partial \bar{x}) ds$$

$$J_{T_2} = 0$$

$$J_{T_3} = \int_{s_2}^{s_3} (-W + \sigma_{\bar{x}\bar{x}} \cdot \partial u_{\bar{x}} / \partial \bar{x}) ds$$

$$J = 2 (J_{T_1} + J_{T_3})$$

Fig.3b: Sketch of the path of integration used

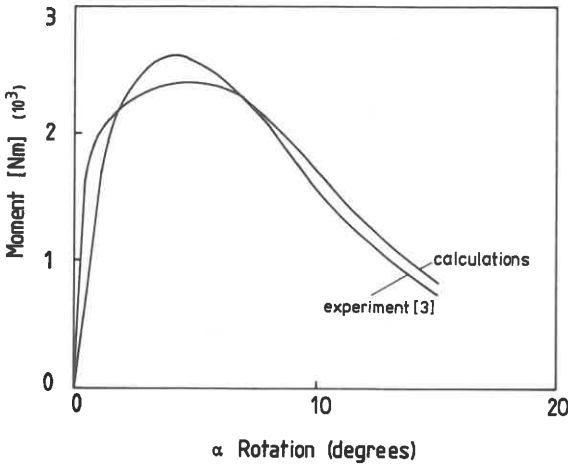


Fig.4: Comparison of moment-rotation curves after the present method with measurements after [3]

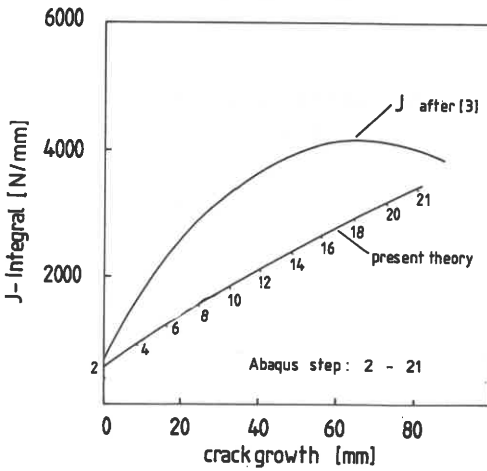


Fig.5: J-integral versus growth of crack length after [3] in comparison with the present theory at "middle of the shell surface"

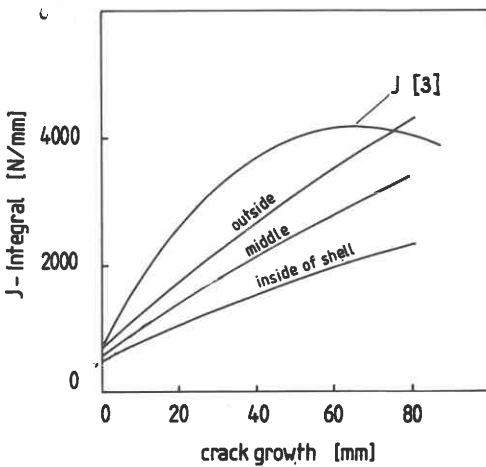


Fig.6: J-integral versus growth of crack length after [3] in comparison with the present method at inside, middle and outside of the shell surface

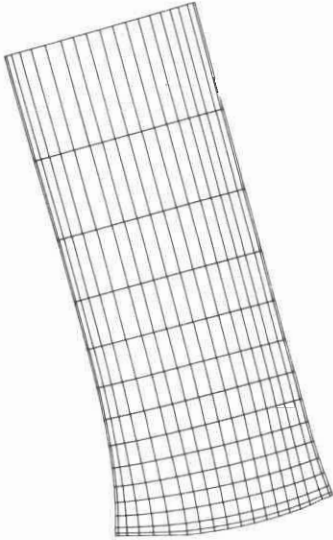


Fig.7:
Plot of the deformed
structure, final stage

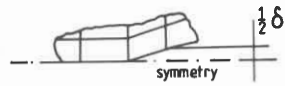
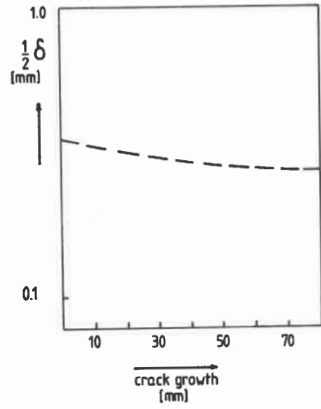


Fig.8:
Crack opening parameter
versus crack growth

APPENDIX :

